

Short Communication

Optimization of Production of Graphene Oxide by Electrochemical Exfoliation: A Response Surface Methodology Application

Yun Yang*, Siyue Zhang, Aiqing Song, Shifang Zhao, Gongfeng Xu

Department of Chemistry College of Biotechnology and Food Science, Tianjin University of Commerce Tianjing, 300134, China

*E-mail: yyun1976@126.com and yyun@tjcu.edu.cn

Received: 4 May 2019 / Accepted: 8 July 2019 / Published: 5 August 2019

Graphene is a two dimensional carbon sheet which is bonded in the hexagonal honeycomb lattice form. In this study, Graphene oxide were produced by electrochemical exfoliation technique and optimized using a response surface methodology application. This study was conducted to evaluate the effect of voltage and pH of H₂SO₄ solution on the mass of graphene flakes. The FESEM and XRD were applied to characterize the structure of produced graphene oxide flakes. The electrochemical impedance spectroscopy results indicated that the reduced graphene oxide had lower charge-transfer resistance. The optimization process was done via Central Composite Design presented in Design expert 10. The optimum conditions were found to be an applied voltage of 9.56 V, and a pH of 1.29. The production optimization using response surface methodology indicated that the combination of the lowest electrolyte pH and the highest voltage applied resulted in the highest mass produced.

Keywords: Graphene oxide; Electrochemical exfoliation; Response surface methodology; Central composite design

1. INTRODUCTION

Graphene is a two-dimensional (2D) reinforced carbon sheet, orchestrated in a hexagonal honeycomb lattice [1]. From a basic perspective, graphene is a solitary layer of graphite. Graphene is a planar monolayer of carbon atom that were separated at 0.142 nm. Graphene also shows promising performance in elasticity, thermal conductivity and high transparency. It has been proven by researchers that graphene has the fastest electron and hole mobility in comparison to other material [2]. Likewise, a solitary layer graphene is a zero-band hole material and exceedingly straightforward, shows optical transmittance of 97.7%. With its high specific surface area of 2600 m²/g, graphene gives an outlook to its performance in the future. One gram of graphene can cover an area of a soccer pitch.

It shows that graphene has an ultimately small size [3].

Graphene researches has guaranteed potential applications including longer-enduring batteries, more proficient sunlight based cells, display panels, and therapeutic advances [4-12]. Numerous researchers have made huge achievement which could be monetarily misused to be actualized in our everyday life. Graphene advancement could affect items in different ventures, from adaptable, wearable, high performance computing to other purposes. The reconciliation of these new materials could convey another measurement to future technologies, where quicker, slenderer, more grounded, adaptable, and broadband gadgets are required [13].

It is very crucial to know that most of the single layer graphene has its own unique properties. The graphene production helps to improve electronic performance, robotics biomechanics and material's mechanical strength. Nevertheless, there is still absence in the graphene sub-atomic functions that can still be studied in the future such as the storage potential and molecular performance [3].

On a bigger scale, graphene is generally acquired from graphite through several methods. The exfoliation and reduction method is the widely-used technique in the industry. Graphene production is normally produced using intercalation and oxidation technique. The graphene intercalation as shown in Figure 1 is further separated into few functionalized graphene [14]. The end products include doping of graphene, pillaring and chemical activation. The method can be visualized in Figure 1.

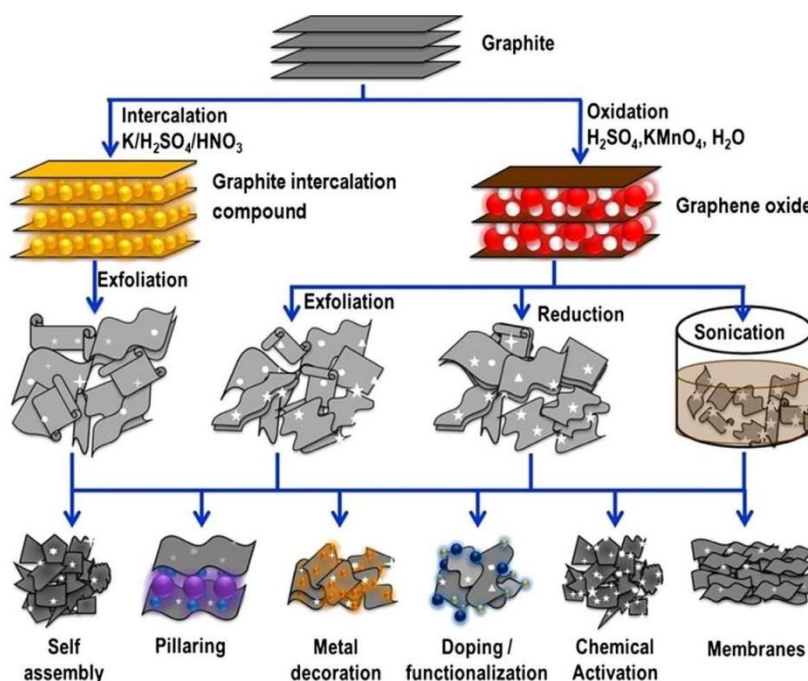


Figure 1. Graphene Production Approach for producing wide variety of graphene based materials in large quantities. [3]

The electrochemical exfoliation reaction experiment mostly done in ionic liquids or acidic

aqueous electrolyte. However, the large quantities production of colloidal graphene in mild or near neutral solution by electrochemical is not always being conducted by the researchers [15].

In a typical electrochemical synthesis of graphene, two electrodes will be used as the cathode and anode. The electrodes can be graphite for both or other than graphite. There are few experiments that have been conducted that uses titanium as the electrode for the electrochemical exfoliation. The electrolyte can be from any acidic aqueous electrolyte. In the previous experiment, researchers used 40 mL aqueous solution with dilution 0.1 M $(\text{NH}_4)_2\text{SO}_4$ as shown in Figure 2. The voltage was set to 10V until all the graphite rod has been exfoliated. As soon as the voltage has been supplied, the graphite starts to exfoliate into small pieces of graphene oxide within an hour. Colloidal graphene ink was prepared by diluting graphene in N-dimethylformamide with a high concentration at sonication state [15].

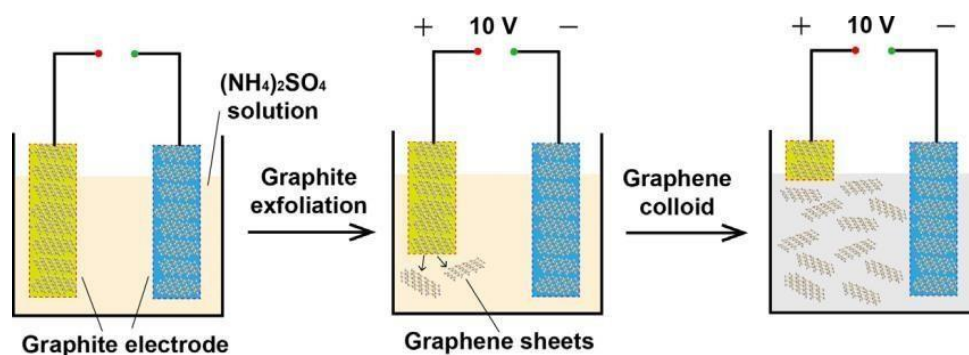


Figure 2. Electrochemical Exfoliation Schematic Diagram [15]

In electrochemical exfoliation, many researchers utilized this method because it is economically wise, fast and environmentally friendly to produce high quality graphene. It has been reported that the method is the best when using H_2SO_4 as the electrolyte in term of exfoliation efficiency [16]. The pH of electrolyte and the voltage applied during experiment also affects the production rate. At low pH, there is a lower percentage of bilayer sheets whereas at voltage larger than 10V results in thick graphene sheets produced [17]. It is shown that the voltage between 6V – 8V is high enough to exfoliate the graphite rod. In this research, authors are comparing all these factors to optimize the process of electrochemical exfoliation [18].

In this research graphene oxide were produced by the electrochemical exfoliation method. We focused on evaluation of the effect of pH and applied voltage on the production rate and investigation of the structure of the graphene flakes produced using FESEM characterization. The optimization utilizes Design of Experiment, Design Expert 10 using Central Composite Design - Response Surface Method. The characterization is limited to FESEM and XRD to characterize the exfoliated graphene oxide flakes.

2. MATERIALS AND METHODS

Natural graphite flakes were used as an electrode and a source of graphene for electrochemical

exfoliation. The graphite flake was followed to a tungsten wire through a silver pad and then was inserted as anode into the ionic solution. Only the graphite was immersed into the electrolyte solution. The ionic solution was prepared by taking 4.8 g of sulfuric acid and diluted in 200 mL of DI water [16, 19]. The electrolyte pH was adjusted from 1 to 3 [2, 17]. A grounded Pt wire was placed parallel to the graphite flake with a separation of 5 cm. The electrochemical exfoliation process was carried out by applying DC bias on the graphite electrode (from 7.5 to 10 V) [15, 17, 20]. To produce the graphene sheet suspension, the exfoliated graphene sheets were collected with a 100 nm porous filter and washed with DI water by vacuum filtration. Then the production was dried using oven at 100 °C for 2 hours to obtain reduced graphene oxide.

Design Expert Software (Version 10, Stat-Ease, Inc., USA) was used to create the regression model and perform statistical and graphical analyses. Thirteen experimental runs were determined from the central composite design (CCD). The values were calculated to run the experiment using Design Expert as shown in Table 1. The mid-point for this experiment has been set to five.

Table 1. Central composite design arrangement for experiment conditions of graphene oxide

Std	Voltage (V)	pH
13	8.50	2.00
12	8.50	2.00
11	8.50	2.00
10	8.50	2.00
9	8.50	2.00
8	8.50	3.00
7	8.50	1.00
6	10.00	2.00
5	7.00	2.00
4	9.56	2.71
3	7.44	2.71
2	9.56	1.29
1	7.44	1.29

Field Emission Scanning Electron Microscope (VP FE-SEM, Carl Zeiss Supra 55 Variable Pressure) Electron microscope was used to characterize graphene powder. X-Ray Diffraction machine (Bruker, model D2 Phaser) was employed to determine the crystallinity of the samples. Citizen CT 53 high precision balance was used to measure mass production. The electrochemical performances involving electrochemical impedance spectroscopy (EIS) were measured by using the Electrochemical Working Station (CHI660D, Shanghai Chenhua, China). The EIS was recorded in the frequency range of 0.1Hz to 0.1 MHz by applying an AC voltage with 5 mV perturbation.

3. RESULTS AND DISCUSSION

The electrochemical exfoliation was studied using Response Surface Design of Experiments.

Design Expert Software was used to create the regression model and perform the statistical and graphical analyses. The experimental applied was a CCD and extended to Response Surface Methodology (RSM) [15]. The response selected is the mass of graphene flakes (mg) production. The factors chosen was the pH level of H₂SO₄ and Voltage applied. Selection of the factors value were determined based on the previous experiments conducted by other researchers. The acidity was selected based on the given properties, thus the lower value was set to pH 1 and the higher value at pH 3. The voltage level was based on the previous experiment. The maximum voltage set was 10 V and the minimum voltage level is 7.5 V [20, 22].

The statistical analysis was applied and the experimental matrix for the design is shown in Table 2. Thirteen experimental was determined by the software from CCD where five runs were determined as the center point. Other values for each run were also indicated in Table 2.

Table 2. Experimental data for the response of the graphene oxide mass production under different extraction conditions

Std	Voltage (V)	Acidity (pH)	Mass (mg)
13	8.50	2.00	12.30
12	8.50	2.00	11.50
11	8.50	2.00	11.60
10	8.50	2.00	11.90
9	8.50	2.00	12.20
8	8.50	3.00	1.00
7	8.50	1.00	80.50
6	10.00	2.00	8.60
5	7.00	2.00	8.10
4	9.56	2.71	7.00
3	7.44	2.71	5.30
2	9.56	1.29	56.00
1	7.44	1.29	34.50

As shown in Table 2, the mass of graphene produced are different for each run. The mass is ranging from 1.00 mg to 80.50 mg for these experiments. The statistical analysis was carried out on these experimental values and the interaction were obtained for the response. The factors and response were obtained by modifying regression analysis to the linear model.

The final equation in terms of actual factors obtained for this model is indicated in the Equation 1. The value of the Standard Deviation, mean and other values can be observed in Table 3.

$$\text{Mass} = -34.68 + 38.50V - 95.30\text{pH} - 6.60V\text{pH} - 1.32V^2 + 29.43\text{pH}^2 \quad (1)$$

Table 3. Experimental Value Analysis of actual factors obtained for regression model

Std. Dev.	5.51		R-Squared	0.9673
Mean	20.04		Adj R-Squared	0.944
C.V. %	27.52		Pred R-Squared	0.768
PRESS	1510.81		Adeq Precision	20.204
-2 Log Likelihood	73.24		BIC	88.63

The quality of the model was confirmed by the R-squared value. R-squared is the square of the correlation between the model's actual values and the predicted values. The square of the correlation ranges from 0 to 1. The greater the R-squared, the better model fit is designated. The statistical significance of the model was assessed using analysis of variance (ANOVA) by the mean square of residual error and regression values. The optimal levels of main parameters and the effects of their interactions on the mass were specified by the CCD of RSM. The ANOVA for the mass indicated that the model was significant as values of Prob > F were less than 0.05, representing that model terms were significant; instead, values of Prob > F larger than 0.05 exhibited that the model terms were insignificant [23]. Indeed, the P-value is the smallest level of significance that might be used to reject the null hypothesis, H_0 . Hence, the smaller the value is, the more significant its corresponding coefficient and the contribution toward the response variable [24]. Insignificant model terms were subsequently removed to improve the model. The ANOVA for the mass shows that the model is significant with the value Prob > F is less than 0.0001. The Model F-value of 41.44 implies the model is significant. There is only 0.01% chance that an F-value could occur due to noise. Prob > F greater than 0.1 showed that the model terms are insignificant [25]. It can be clearly seen in the ANOVA for the mass response in Table 4.

Table 4. Analysis of variance of the factors and the critical values obtained from the response surface for the mass production of graphene oxide

Source	Sum of Squares	df	Mean Square	F Value	Prob > F	Comment
Model	6299.84	5	1259.970	41.44	0.00005	significant
A-Voltage	71.44	1	71.440	2.35	0.16918	
B-Acidity	4542.47	1	4542.470	149.39	0.00001	
AB	98.01	1	98.010	3.22	0.11567	
A ²	15.39	1	15.390	0.51	0.49980	
B ²	1505.79	1	1505.790	49.52	0.00020	
Residual	212.85	7	30.410			

The interaction between two factors on the mass produced shows that the gradient when pH=1.29 is higher compared to when the pH=2.71. At higher pH, it is observed that the graph displayed is almost like the straight line which shows high pH value is a major drawback to the mass

produced.

At lower pH the result is very promising due to the high concentration of H^+ present in the electrolyte. At pH=1.29 it can produce a minimum mass of approximately 36 mg using only the voltage of 7V. At Voltage=9.56 and pH=1.29, the mass produced is 56 mg.

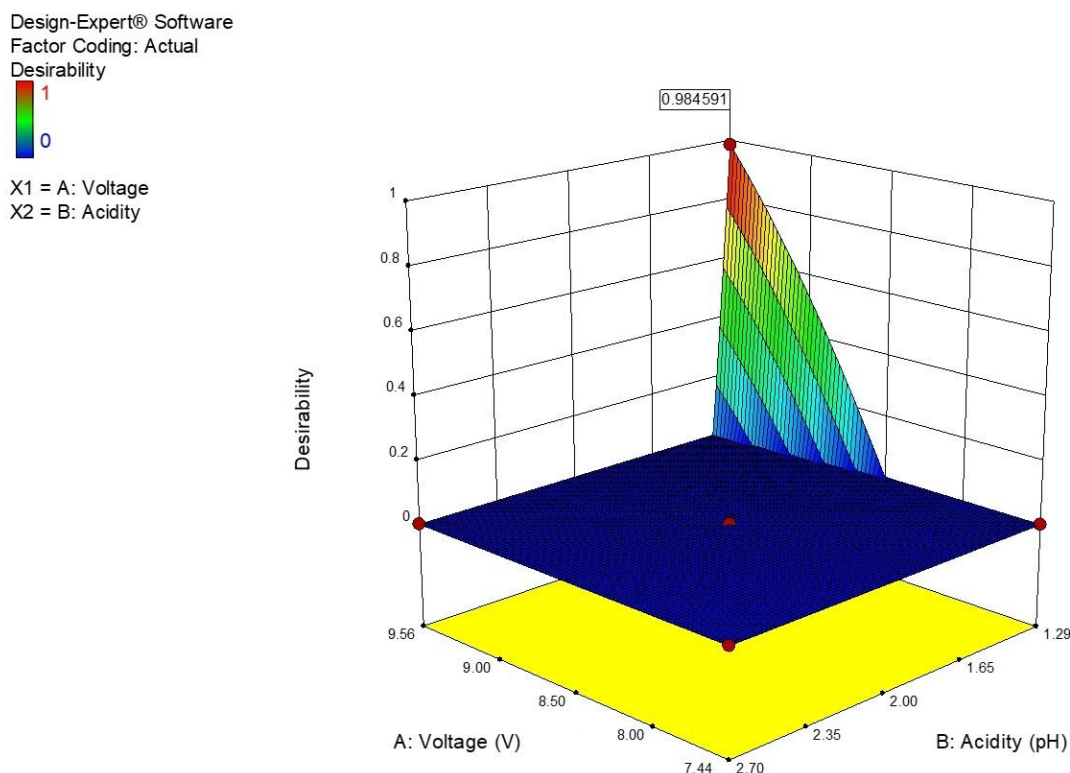


Figure 3. Desirability 3D Response Surfacing of electrolyte acidity and voltage on the mass production of graphene oxide

It is observed that the maximum possible mass is 56.89 mg. The voltage required to achieve this result is 9.56 V and the acidity required is 1.29 pH. The desirability for this run is 0.985 as shown in Figure 3 which is considered promising for the experiment. The Desirability 3D Surface can be analyzed in Figure 3 that exhibit the desirability of each run.

In order to verify the graphene oxide flakes FESEM was selected to confirm the morphological properties. Figure 4 exhibits the image of graphene oxide at magnification of 5000 times. The graphene oxide is seen as a chunk. It shows that the exfoliated layers of graphene oxide are stacked together. The stacked graphene oxide is due to its powder form. There is no crystalline structure for graphene oxide because of the atomic arrangement. It is observed that there is no uniform distribution of size and shape of graphene oxide which can be attributed to the deformation during exfoliation and restacking process of graphene oxide after some time. As graphene oxide is the stacked layers of graphite, we can see the white lines indicating its folded structure.

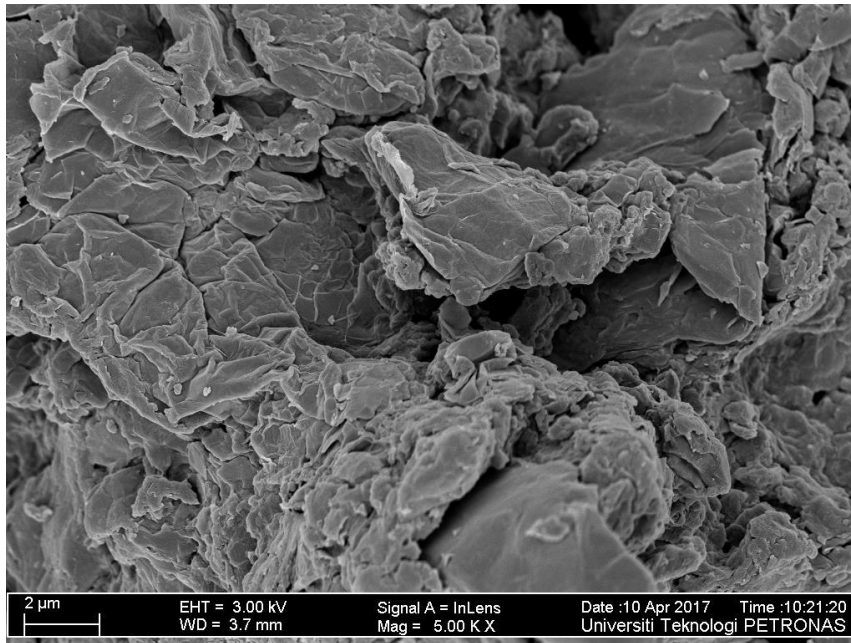


Figure 4. Typical FESEM image for an electrochemically exfoliated graphene oxide thin sheet at the voltage of 9.56 V and the acidity pH of 1.29

X-Ray Diffraction is the rapid analytical technique and procedures to identify the element present in the sample. The peak obtained from the XRD graph is compared to the Joint Committee on Powder Diffraction Standards (JCPDS) card database to determine the content of the sample. Figure 5 is the raw XRD pattern of exfoliated graphene oxide.

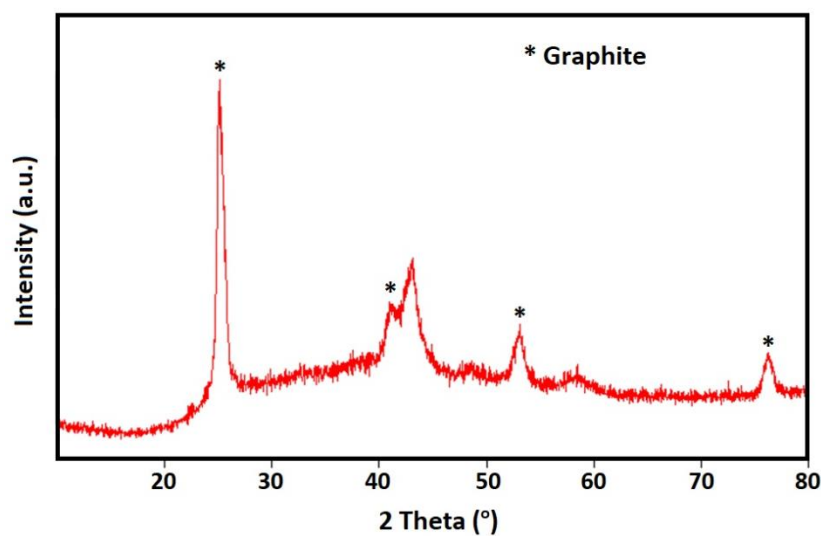


Figure 5. XRD Pattern of electrochemically exfoliated graphene oxide at the voltage of 9.56 V and the acidity pH of 1.29

XRD pattern shows the structure of graphene oxide has a sharp peak at $2\theta=24.995^\circ$ which is in accordance to JCPDS card of (00-001-0646) Graphite.

For this particular sample, there are 34% crystallinity and 66% amorphous. It is due to high water molecule content in the sample. The effect of placing the sample at room condition is not recommended because the sample will absorb air particles around them that will result in high amorphous solid.

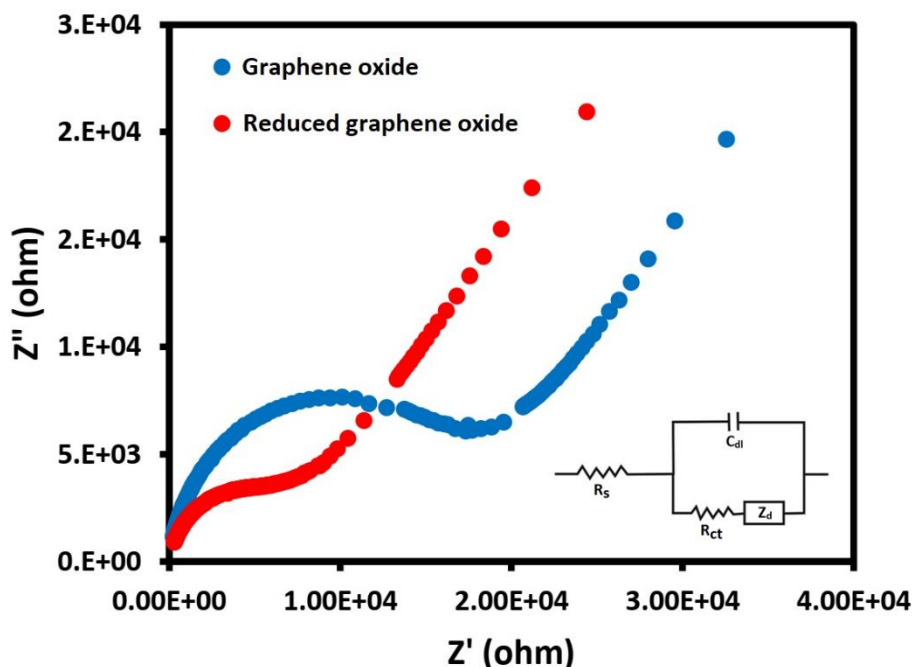


Figure 6. EIS plots of graphene oxide and reduced graphene oxide (inset indicates the electrochemical equivalent circuit model).

Nyquist plots are utilized to analyze the EIS data and indicate with the equivalent circuit as shown in Figure 6. In the high frequency region, the real axis intercept represents a combined resistance (R_s) containing ionic resistance of electrolyte, intrinsic resistance of electrode materials, and contact resistance between the current collector and electrode [26, 27]. Furthermore, the semicircle radius is revealing of the charge-transfer resistance (R_{ct}) of electrode materials and the electrode conductivity [28]. The EIS plots demonstrate identical R_s for reduced graphene oxide approximately 6.86Ω , which is larger than that of graphene oxide (4.69Ω). And the fitted values of R_{ct} attain for graphene oxide and reduced graphene oxide are $7.51 \text{ k}\Omega$ and $3.64 \text{ k}\Omega$, respectively. It can be attributed to the formation of defects on the surface of electrodes during preparation by using an electrochemical exfoliation process. In the intermediate frequency region, the 45-degree line, also known as the Warburg element in the equivalent circuit [29], which represents the ion diffusion/transport in the electrolyte.

4. CONCLUSION

In this research, the Design of Experiment was successfully utilized to optimize the production of graphene oxide produced by electrochemical exfoliation. The FESEM image obtained proves that the graphene oxides flakes are stacked in layers. XRD pattern of the graphene oxide is in accordance with FESEM findings. The EIS plots the fitted values of R_{ct} attain for graphene oxide and reduced graphene oxide are 7.51 k Ω and 3.64 k Ω , respectively. It can be attributed to the formation of defects on the surface of electrodes during preparation by using an electrochemical exfoliation process. The production optimization using Response Surface Method was successful where the combination of lowest pH and highest voltage gave the best result. The optimum conditions were found to be an applied voltage of 9.56 V, and a pH of 1.29. The results show that it can be introduced as a continuous research because there is always alternative to improve the graphene production.

ACKNOWLEDGEMENTS

This work was funded by School Training Programs of Innovation and Entrepreneurship for Undergraduates (201910069169).

References

1. D. Jiang, L. Liu, G. Wu, Q. Zhang, J. Long, Z. Wu, F. Xie and Y. Huang, *Polymer Composites*, 38 (2017) 2425.
2. R.I. Jibrael and M.K. Mohammed, *Optik*, 127 (2016) 6384.
3. S. Gadipelli and Z.X. Guo, *Progress in Materials Science*, 69 (2015) 1.
4. M.J. Loveridge, M.J. Lain, Q. Huang, C. Wan, A.J. Roberts, G.S. Pappas and R. Bhagat, *Physical Chemistry Chemical Physics*, 18 (2016) 30677.
5. L.M. Yang, Z.L. Chen, D. Cui, X. B. Luo, B. Liang, L.X. Yang, T. Liu, A. J. Wang and S. L. Luo. *Chem. Eng. J.*, 359(2019)894.
6. S. Guo, S. Dong, E. Wang, *ACS Nano.*, 4 (2009) 547–555.
7. P. H. Shao, J. Y. Tian, F. Yang, X. G. Duan, S. S. Gao, W. X. Shi, X. B. Luo, F. Y. Cui, S. L. Luo and S. B. Wang, *Adv. Funct. Mater.*, 28 (2018) 1705295.
8. S. F. Tang, D. L. Yuan, Y. D. Rao, M. H. Li, G. M. Shi, J. M. Gu and T. H. Zhang. *J. Hazard. Mater.*, 366 (2019) 669.
9. H. Y. Yu, P. H. Shao, L. L. Fang, J. J. Pei, L. Ding, S. G. Pavlostathis and X. B. Luo, *Chem. Eng. J.*, 359 (2019) 176.
10. Q.Zhang,S.Bolisetty, Y.Cao,S.Handschin,J.Adamcik,Q.Peng,R.Mezzenga, *Angew. Chem.-Int. Edit.*,58(2019)6012.
11. M. Xu, J. Qi, F. Li and Y. Zhang, *Journal of materials science*, 53 (2018) 9589.
12. R. Kurapati, K. Kostarelos, M. Prato and A. Bianco, *Advanced Materials*, 28 (2016) 6052.
13. F. Bonaccorso, L. Colombo, G. Yu, M. Stoller, V. Tozzini, A.C. Ferrari, R.S. Ruoff and V. Pellegrini, *Science*, 347 (2015) 1246501.
14. M. Matsumoto, Y. Saito, C. Park, T. Fukushima and T. Aida, *Nature chemistry*, 7 (2015) 730.
15. K. Chen and D. Xue, *Journal of colloid and interface science*, 436 (2014) 41.
16. J. Liu, C.K. Poh, D. Zhan, L. Lai, S.H. Lim, L. Wang, X. Liu, N.G. Sahoo, C. Li and Z. Shen, *Nano Energy*, 2 (2013) 377.
17. P. Yu, S.E. Lowe, G.P. Simon and Y.L. Zhong, *Current opinion in colloid & interface science*, 20 (2015) 329.
18. C.-Y. Su, A.-Y. Lu, Y. Xu, F.-R. Chen, A.N. Khlobystov and L.-J. Li, *ACS nano*, 5 (2011) 2332.

19. C.-H. Chuang, C.-Y. Su, K.-T. Hsu, C.-H. Chen, C.-H. Huang, C.-W. Chu and W.-R. Liu, *RSC Advances*, 5 (2015) 2015.
20. K. Chen, D. Xue and S. Komarneni, *Journal of colloid and interface science*, 487 (2017) 156.
21. J. Rouhi, S. Mahmud, S. Hutagalung and S. Kakooei, *Micro & Nano Letters*, 7 (2012) 325.
22. J. Liu, H. Yang, S.G. Zhen, C.K. Poh, A. Chaurasia, J. Luo, X. Wu, E.K.L. Yeow, N.G. Sahoo and J. Lin, *Rsc Advances*, 3 (2013) 11745.
23. S. Srivastava and R. Garg, *Journal of Manufacturing Processes*, 25 (2017) 296.
24. H. Mazaheri, K.T. Lee, S. Bhatia and A.R. Mohamed, *Bioresource technology*, 101 (2010) 745.
25. J. Rouhi, S. Mahmud, S.D. Hutagalung, N. Naderi, S. Kakooei and M.J. Abdullah, *Semiconductor Science and Technology*, 27 (2012) 065001.
26. D. Li, Y. Gong and C. Pan, *Scientific reports*, 6 (2016) 29788.
27. Q. Fang and S. Li, *International Journal of Electrochemical Science*, 14 (2019) 5042.
28. M. Husairi, J. Rouhi, K. Alvin, Z. Atikah, M. Rusop and S. Abdullah, *Semiconductor Science and Technology*, 29 (2014) 075015.
29. N.H. Basri, M. Deraman, M. Suleman, N.S.M. Nor, B.N.M. Dolah, M.I. Sahri and S.A. Shamsudin, *International Journal of Electrochemical Science*, 11 (2016) 95.

© 2019 The Authors. Published by ESG (www.electrochemsci.org). This article is an open access article distributed under the terms and conditions of the Creative Commons Attribution license (<http://creativecommons.org/licenses/by/4.0/>).